

Analysis of Electromagnetic Conditions Around the Conductor Clamp of a Covered Conductor

Abstract. The paper brings analyses of electromagnetic conditions around conductor clamp of ceramic insulator used in medium voltage networks with covered conductors. The objective of the analyses performed was to investigate the reasons of frequent damages of conductor clamps, covered conductors' insulation or the conductors themselves in the area of the conductor clamp. The analyses were performed on an insulator made by one of commercial manufacturers of electrical equipment using the Opera Vector Fields program tool, which uses 3D finite elements method. The paper also includes a description of comparisons of conditions for various materials of conductor clamps with the same shape. For all the examples investigated, it also contains the distributions of electric field in the insulator and its surroundings, as well as eddy currents in the nearby metal parts. Thus, the importance of adequate selection of materials of conductor clamps is demonstrated, since inadequate selection can due to electrical burden lead to serious damage. On the basis of the results obtained a technical solution that reduces possibility of damage is proposed.

Streszczenie. W pracy przedstawiono analizy warunków elektromagnetycznych wokół zacisku przewodu izolatora ceramicznego stosowanego w sieciach średniego napięcia z osłoniętymi przewodnikami. Celem przeprowadzonych analiz było zbadanie przyczyn częstych uszkodzeń zacisków przewodów, pokrycia izolacji przewodów lub samych przewodów w obszarze zacisku przewodu. Analizy przeprowadzono na izolatorze wykonanym przez jednego z komercyjnych producentów sprzętu elektrycznego za pomocą programu Opera Vector Fields, wykorzystującego metodę elementów skończonych 3D. Artykuł zawiera również opis porównań warunków dla różnych materiałów zacisków przewodnika o tym samym kształcie. Dla wszystkich zbadanych przykładów zawiera również rozkłady pola elektrycznego w izolatorze i jego otoczeniu, a także prądy wirowe w pobliskich częściach metalowych. W związku z tym wykazano znaczenie odpowiedniego doboru materiałów na zaciski przewodów, ponieważ nieodpowiedni wybór może ze względu na obciążenie elektryczne prowadzić do poważnych uszkodzeń. Na podstawie uzyskanych wyników zaproponowano rozwiązanie techniczne, które ogranicza możliwość uszkodzenia. (Analiza warunków elektromagnetycznych wokół zacisku przewodu w osłoniętym przewodzie)

Keywords: insulators, conductor clamps, covered conductors, electromagnetic conditions, partial discharge

Słowa kluczowe: izolatory, zaciski przewodów, przewody osłonięte, warunki elektromagnetyczne, wyładowania niepełne

Introduction

Electric insulators are almost indispensable parts of each electric power network. Development of materials constantly brings new insulators with better insulation and mechanical properties. In the recent years, covered conductors that have many advantages and contribute to increased security of network operation often replace bare conductors. Covered conductors also have some disadvantages, such as inefficient performance of protection systems, difficult location of faults [1], insulation damage due to corona [2], [3], danger for people in the case of a fall of conductor to the ground, if the conductor remains energized, etc.

The most frequent problems with covered conductors appear at the points of fixing the conductor to insulator [4], [5]. The reasons of these problems are usually inadequate combinations of properties of materials that compose conductor clamps. In most cases, they are composed of several materials with different dielectric constants with some metal parts between them. Inadequate geometrical forms of components of conductor clamps additionally worsen the situation.

The paper presents the results of analyses of electromagnetic conditions in a »D-type« pin insulator, model »VS SER-b/20«, with metal conductor clamp and the use of covered conductor [6], [7]. The numerical computations of conditions inside the insulator and its surroundings were performed using Opera Vector Fields 3D program tool [9]. Computations of electrostatic and time-harmonic electromagnetic field were performed for different materials of components of conductor clamps having the same shape [8]. The influence of various materials is evident from the differences in electric field distribution in and around the insulator and eddy currents in the nearby metal parts. An accurate analysis of electric field calculation results also enabled identification of conditions that lead to damaging of conductor clamps and conductors.

Description of damages to conductor clamp and conductor

The details about the insulator with conductor clamp for covered conductors, which was used for the analyses of electric and magnetic conditions, are shown in Fig. 1. Damages that appear most frequently on this type of insulators are caused by partial discharges between metal part of the conductor clamp and insulation of the covered conductor. These discharges during the course of the time cause erosion of metal parts of the conductor clamp, as well as of insulation and metal parts of the covered conductor. An example of such damage is shown in Fig. 2.



Fig. 1: Metal conductor clamp of covered conductor on which the analyses were performed.



Fig. 2: Two examples of damages to insulation of covered conductor and conductor clamp.

The geometrical and mathematical model use in numerical computations

3D geometrical model that was used in analyzing electromagnetic conditions is an accurate model of the

actual insulator, conductor clamp and a part of covered conductor. The cross-section of the model is with the labeled components shown in Fig. 3.

This type of insulators is use in 3-phase medium voltage AC networks with nominal phase-to-phase RMS voltage 20 kV. Electromagnetic field computations were performed for maximum operating voltage of the insulator, which in these networks amounts to 24 kV. Input parameters in the computations were peak values of electric potential on the conductor and on the pin. Since the pin is galvanically connected with the supporting pillar, its potential V_b equals to 0 V. The insulator is in this case located in the electric field of phase voltage; therefore can be expressed as (1).

$$(1) \quad V_c = \frac{\sqrt{2}}{\sqrt{3}} \cdot 24 \cong 19.6 \text{ kV}$$

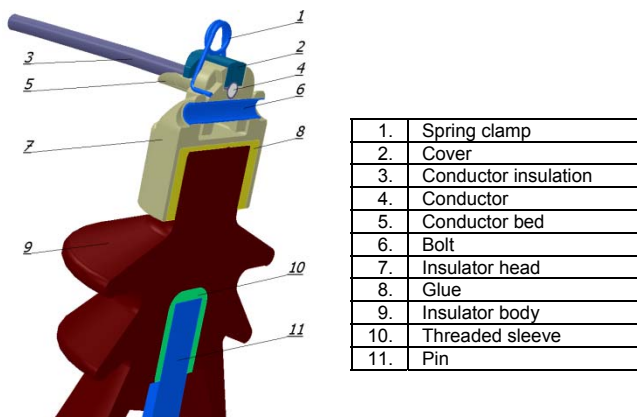


Fig. 3: Components of ceramic pin insulator VS SER – b/20.

The points of electric potential that were in numerical computations set as boundary conditions can be seen in Fig. 4a, while Fig. 4b shows the applied discretization of the geometrical model.

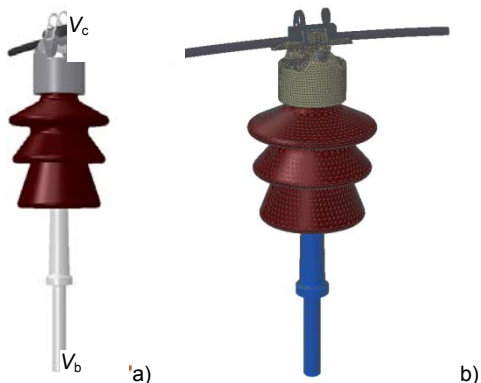


Fig. 4: Determination of potential and discretization used in electric field computations.

The analysis of electromagnetic conditions in the insulator and its surroundings was performed using two methods. In the first method, static electric field was calculated based on Poisson's equation (2).

$$(2) \quad \nabla \cdot \varepsilon \nabla V = -\rho$$

In the equation ε is dielectric constant of the material, V is electric potential, while ρ is electric charge density. In the case of known distribution of electric potential V , the electric field strength E is calculated using (3).

$$(3) \quad E = -\nabla V$$

In the second method of analysis, a harmonic steady state magnetic field was computed. The electromagnetic conditions for this case are described by the equations (4) and (5).

$$(4) \quad \nabla \times \frac{1}{\mu} \nabla \times A + j\omega \sigma A + \sigma \nabla V = 0$$

$$(5) \quad \nabla \cdot \sigma \nabla V + j\omega \nabla \cdot \sigma A = 0$$

where A is magnetic vector potential, μ is permeability, ω is angular frequency, while σ is electric conductivity.

All electromagnetic field computations were performed on the same geometrical model of the insulator, which had three different versions. The versions differentiated from each other by the type of material components of the conductor clamps on the insulator:

- a) All parts of the conductor clamp are metal, except the cover that is made of bakelite (Fig. 5a);
- b) All parts of the conductor clamp are plastic (of PA6), except spring and bolt, which are metal (Fig. 5b); and
- c) All parts of the conductor clamp are plastic (of PA6), except spring, which is metal (Fig. 5c)

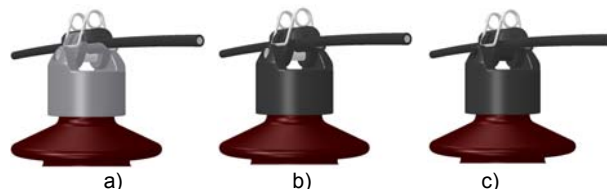


Fig. 5: Different versions of studied conductor clamps.

Table 1 gives the properties of materials used in electromagnetic field computations for different versions.

Table 1. Data on the materials used in electromagnetic field computations.

Version	Part of Insulator	Material	Relative dielectric constant ε_r	Dielectric strength E_p (MV/m)	Relative permeability μ_r	Electric conductivity σ (S/m)
	Spring clamp	Steel	/	/	300	$9.9 \cdot 10^8$
	Conductor insulation	XLPE	2.5	30 - 50	1	10^{-15}
	Conductor	Al-Mg-Si	/	/	1	$33.3 \cdot 10^8$
	Glue	Epoxy	5	10 - 30	1	10^{-11}
	Threaded sleeve	Pb-Sb	/	/	/	$4.6 \cdot 10^7$
	Insulator body	El. porcelain	6.5	30 - 35	1	10^{-11}
	Pin	Steel	/	/	6000	$1.1 \cdot 10^7$
a)	Cover	Bakelite	4.6	30	1	10^9
	Conductor bed	Al-Mg-Si	/	/	1	$30.3 \cdot 10^8$
	Insulator head	Al-Mg-Si	/	/	1	$30.3 \cdot 10^8$
	Bolt	Steel	/	/	300	$9.9 \cdot 10^8$
b)	Cover	PA6	3.2	30	1	10^{10}
	Conductor bed	PA6	3.2	30	1	10^{10}
	Insulator head	PA6	3.2	30	1	10^{10}
	Bolt	Steel	/	/	300	$9.9 \cdot 10^8$
c)	Cover	PA6	3.2	30	1	10^{10}
	Conductor bed	PA6	3.2	30	1	10^{10}
	Insulator head	PA6	3.2	30	1	10^{10}
	Bolt	PA6	3.2	30	1	10^{10}

Results of electromagnetic field computations

Computation of electrostatic field

The computation of static electromagnetic field was performed for the case where the entire metal part of the conductor had electric potential of 19.6 kV, while the fixing pin was on 0 V. The distribution of electric potential in the upper part of the insulator for all three versions of conductor clamp is shown in Fig. 6, while the distribution of electric field strength on the surface of the conductor clamp's components is shown in Fig. 7.

From Fig. 6 it is evident that electric potential in versions **b)** and **c)** decreases with distance much more rapidly than in version **a)**. The conductor bed (5 in Fig. 1) is thus in conductor clamp versions **b)** and **c)** on higher electric potential than in version **a)** (Fig. 6), which means that the insulation is under lower electric stress. This is also

confirmed by the distributions of electric field strength in Fig. 7. From it is also evident that in version **a)** electric field strength at the conductor surface reaches up to 2.7 MV/m. This value does represent a threat to the conductor insulation made of XLPE (Cross-linked polyethylene), since it, dielectric strength lies in the range between 30 and 50 MV/m.

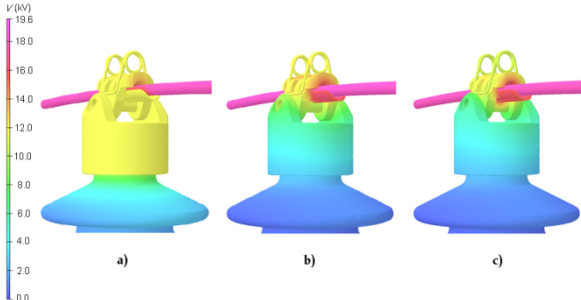


Fig. 6: Distribution of electric potential in the upper part of insulator and conductor clamp.

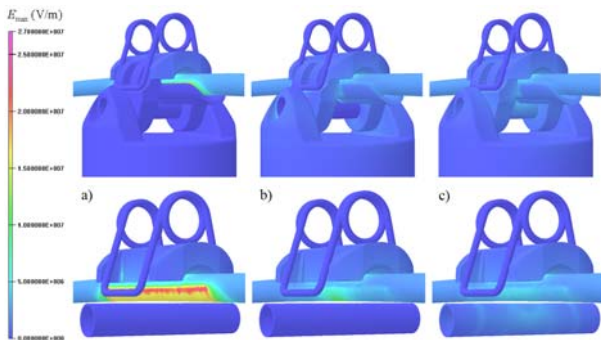


Fig. 7: Electric field strength on the surface of conductor clamp and conductor insulation

Electric stresses of the internal part of the conductor clamp are for the selected cross section shown in Fig. 8. The cross section 1 was selected in the center of the conductor clamp, cross section 2 is for 44 mm distant from the center in the direction of the conductor, while the cross section 3 was selected in the axis of the conductor.

From Fig. 9 it is evident that in the version **a)**, i.e. insulator with metal conductor clamp, the electric field strength in the air gap between the conductor insulation and the conductor bed is much higher than in versions **b)** and **c)**. This value exceeds the electric field strength of air which amounts to 3 MV/m.

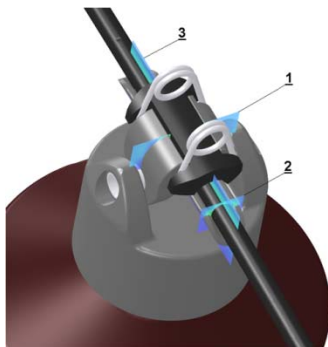


Fig. 8: Positions of cross-sections of presentation of electric field strength: 1) Cross section in the center of conductor clamp, 2) Cross section 44 mm from the center and 3) Longitudinal section by the conductor axis.

The same problem appears in the version **b)** where the values of electric field strength exceed dielectric strength of air in the area between the bolt and the head of conductor clamp. In this case partial discharges are also possible,

which may cause erosion of surrounding parts. In the version **c)** electric field strength is on the whole cross-section lower and in areas filled with air never exceeds 1.5 MV/m, which is well below the dielectric strength of air. The distribution of electric field that is shown in Fig. 9c was computed using relative dielectric constant of the cover $\epsilon_{r \text{ cover}} = 3.2$. If relative dielectric constant is increased to $\epsilon_{r \text{ cover}} = 5.5$, electric field strength in the air gap between conductor and the cover rises to 4.34 MV/m, which is already higher than the dielectric strength of air.

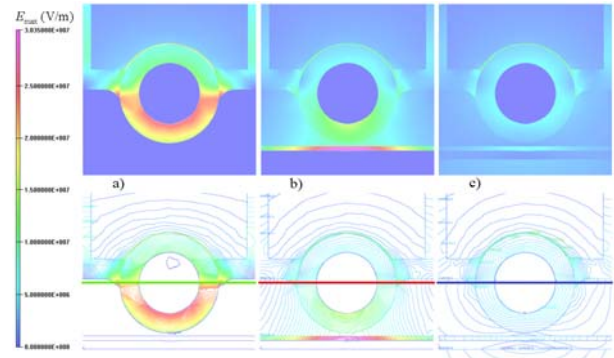


Fig. 9: Distribution of electric field strength in the transverse cross-section 1 (Fig. 8).

In the area of cross-section 2 the cover no longer covers the conductor. This cross-section is also so distant from the bolt that the bolt material has no impact on the electric field. In the version **a)** also at this point electric field strength in the air gap between conductor bed and conductor exceeds dielectric strength of air, while for versions **b)** and **c)** it stays below this value.

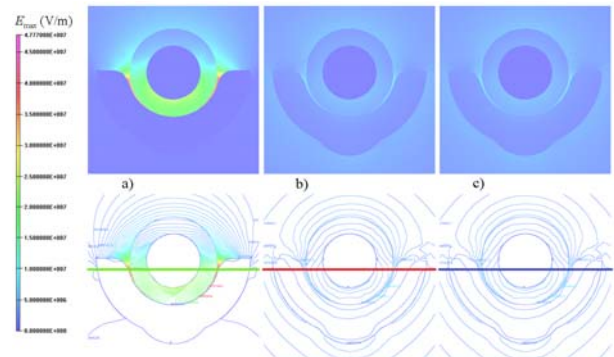


Fig. 10: Electric field strength in the transverse cross-section 2 (Fig. 8).

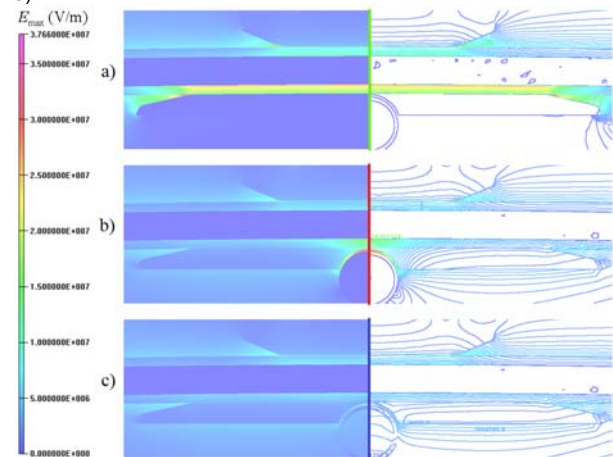


Fig. 11: Electric field strength in longitudinal cross-section 3 (Fig. 8).

The distribution of electric field strength in the longitudinal cross-section 3 (Fig. 8) is shown in Fig. 11. This figure confirms findings from Fig. 9 and Fig. 10.

Computation of harmonic electromagnetic field

The computation of electromagnetic field was performed for the case of version with metal conductor clamp, since only in this versions eddy currents have an important impact on electromagnetic field. The peak value of current through the conductor amounted to 25.7 A, and was changing over time in accordance with cosine function. The magnetic and electric properties of materials used in the computations are given in Table 1.

The distribution of electric magnetic flux density in the moment $\Delta t = 0^\circ$ is shown in Fig. 12. Due to temporal variations of magnetic conditions eddy currents are induced in the conductive parts of conductor clamp. These currents reach maximum values at $\Delta t = 90^\circ$. The distribution of their density and direction is shown in Fig. 13.

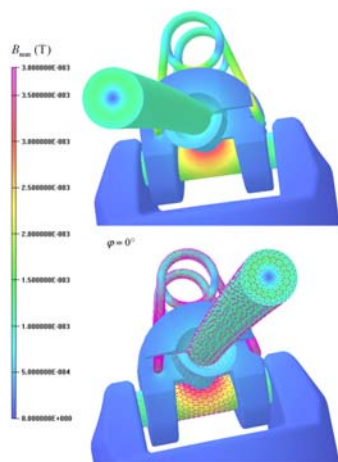


Fig. 12: Distribution of magnetic flux density and its direction at $\Delta t = 0^\circ$.

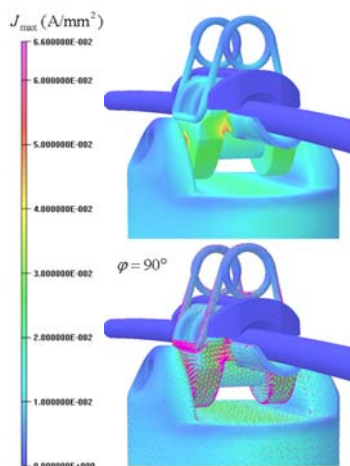


Fig. 13: Distribution of current density and its direction at $\Delta t = 90^\circ$.

As it is evident from Fig. 12 and Fig. 13 the values of magnetic and current flux densities are low, which means that they do not cause any damage on the conductor clamp of covered conductors.

Conclusions

For the computation of electromagnetic conditions in the conductor clamp of covered conductor the Vector – Fields Opera 3D program tool based on FEM was used. Due to complex geometric forms of the conductor clamp's

components, it is not possible to mode electromagnetic conditions using conventional analytic procedures.

From the results of the computations, it is possible to draw conclusion electric potential on the insulator with conductor clamp made of insulating material decreases faster than on the insulator with conductor clamp made of conducting material. The combined metal-plastic conductor clamp is at unchanged geometry practically useless, since in the air gap between the conductor bed and metal bolt there is excessive electric field strength that would cause discharges in this area. The computations performed confirm that the most suitable conductor clamp is made of plastic parts. In this case, electric stress is evenly distributed among all parts of the conductor clamp and insulator's body. The values of electric field strengths in the air gap between the conductor's insulation and conductor bed of the conductor clamp and in the air gap under the cover are in this case at the case of nominal voltage within the allowed interval.

By replacing the metal part of the conductor clamp by one made of insulation material, the stress caused by electric field strength is reduced, which prolongs the lifetime of insulator and covered conductor. This intervention also reduces losses in the insulator since the appearance of eddy currents is thus prevented.

Authors: prof. dr. Anton Hamler, UM FERi, Koroška cesta 46, 2000 Maribor, Slovenia, E-mail: anton.hamler@um.si; doc. dr Miloš Beković, UM FERi, Koroška cesta 46, 2000 Maribor, Slovenia, E-mail: milos.bekovic@um.si;

REFERENCES

- [1] S. Misak, S. Hamacek, P. Bilik, M. Hofinek, P. Petvaldsky, "Problems Associated With Covered Conductor Fault Detection", International Conference on Electrical Power Quality and Utilisation (EPQU), 17-19 Oct. 2011.
- [2] T. Yamashita, T. Ishihara, M. Kawaguchi, T. Fujishima, H. Matsuo, and M. Furuta, "Detrioration of insulated wire by corona discharge", *Inst. Elect. Eng. J. Trans. Power Energy*, vol. 126, no. 12, 2006.
- [3] P. Heine, J. Pitkänen, M. Lehtonen: "Voltage Sag Characteristics of Covered Conductor Feeders", 38th International Universities Power Engineering Conference, UPEC 2003, Thessaloniki, Greece, September 1-3, 2003.
- [4] G. Ban, L. Prikler, I. Fogarasi, I. Hajos, "Protection of MV Covered Conductor Lines against Overvoltages and Fault Arcs", *Power Tech*, 2005 IEEE Russia, 27-30 June 2005.
- [5] N. Solís, J. A. Gutiérrez, J. L. Naredo, V. H. Ortiz, "Analysis of complex faults in distribution systems", International Conference on Power Systems Transients (IPST'07), Lyon, France, 4-7 June, 2007.
- [6] J. Pihler, I. Tičar, "Design of Systems of Covered Overhead Conductors by Means of Electric Field Calculation", *IEEE Transactions on power delivery*, Vol. 20, No. 2, pp. 807-814, April 2005.
- [7] P. Urbanec, "The Analysis of electromagnetic conditions in the insulator and the surrounding area by using of covered conductor", Diploma thesis, Univ. Maribor, Faculty of Elect. Eng. & Comput. Sci., Maribor, Slovenia, 2010.
- [8] E. A. Bauer: "Plastic Composite insulators to the system Rodurflex", Presentation to the IEEE Nonceramic/Composite Insulator Working group in New York, January 28, 1976.
- [9] Opera - 3d Reference manual, version 13.014, december, 2009.